Selective strong-field enhancement and suppression of ionization with short laser pulses

N. A. Hart,[1,*] J. Strohaber,[2] A. A. Kolomenskii,[1] G. G. Paulus,[3] D. Bauer,[4] and H. A. Schuessler[1]
[1]*Department of Physics, Texas A&M University, College Station, Texas 77843, USA*
[2]*Department of Physics, Florida A&M University, Tallahassee, Florida 32307, USA*
[3]*Institut fuer Optik und Quantenelektronik, Friedrich-Schiller-Universitaet Jena, Max-Wien-Platz 1, 07743 Jena, Germany*
[4]*Institut fur Physik, Universty of Rostock, 18051 Rostock, Germany*
(Received 30 October 2015; published 28 June 2016)

We experimentally demonstrate robust selective excitation and attenuation of atomic Rydberg level populations in sodium vapor (Na I) using intense laser pulses in the strong-field limit ($>10^{12}$ W/cm^2). Coherent control of the atomic population and related ionization channels is realized for intensities above the over-the-barrier ionization intensity. Moreover, atomic excitation selectivity and high ionization yield are simultaneously achieved without the need to tailor the spectral phase of the laser. A qualitative model confirms that this strong-field coherent control arises through the manifestation of a Freeman resonance.

DOI: 10.1103/PhysRevA.93.063426

I. INTRODUCTION

Practical implementation of resonantly enhanced multiphoton ionization (REMPI) in the strong-field limit is complicated because of nonstatic intermediate resonances [1]. This is due to dynamic Stark shifts and Stark splittings that satisfy an integer-photon resonance in an intensity-dependent manner [2,3]. For a dipole transition, requiring at least K photons, perturbation theory predicts that the photon absorption rate W is proportional to the intensity I to the Kth power ($W \propto I^K$). However, using cesium (Cs) atoms, Held *et al.* [4] showed experimentally and Chang and Stehle [5] demonstrated theoretically that a four-photon ionization can have a $K \equiv \log(W)/\log(I)$ value as low as 1 and as high as 8, depending on the amount of laser frequency detuning from the resonance. In this case, K no longer simply represents the multiphoton order.

Freeman *et al.* [6] discovered that when atomic Rydberg states transiently Stark-shift into resonance, they can be energetically resolved in the photoelectron yield. Observation of the effect requires the pulse duration to be shorter than the time it takes emitted electrons to exit the laser focus, and the laser bandwidth to be smaller than the spacing between excited energy levels. This dynamic shift into resonance, commonly referred to as "Freeman resonance," is an important and pervasive phenomenon in strong-field physics. This is partly because it satisfies the condition for REMPI and is therefore associated with enhanced coherent ionization [6,7].

One critically important problem for the strong-field coherent control of REMPI is how to selectively ionize through a single energy level and produce high ion yields simultaneously. While increasing laser intensity can increase yields, it can also spread the electron population across multiple energy levels [7]. This in turn reduces selectivity of the ionization channel and decreases ionization efficiency due to high-field stabilization [8]. Here we demonstrate that by using the appropriate laser wavelength and intensity, improved selectivity and yield can be obtained by a simple mechanism. In contrast to previous experiments [9], we control the ac Stark shift in atomic sodium by changing the intensity of an unshaped femtosecond laser pulse. This allows us to discriminate between multiphoton resonances in a manifold of sodium Rydberg P states. By satisfying only one Freeman resonance of the manifold at the peak of the pulse (where nonlinear effects are maximum), REMPI through this resonance is selectively enhanced, while other ionization channels are simultaneously suppressed.

II. EXPERIMENTAL SETUP

Details of our experimental equipment have been described previously [10]. Briefly, our Ti:sapphire laser system produced 57-fs pulses with a center wavelength of 800 nm. A photodiode (PD) detected pulses from leakage through a steering mirror (M) and was used to trigger data-acquisition software (see Fig. 1). The power attenuator was a two-component device composed of a rotatable half-wave plate that changed the polarization of the laser beam and a fixed polarizing beam-splitter cube that filtered out vertically polarized radiation while passing the horizontal. The sodium oven was located within the vacuum chamber. The oven temperature was maintained at 256 °C producing a Na vapor density of 2×10^{14} cm^{-3} at the oven exit and a density of 5×10^{13} cm^{-3} ($\sim 3 \times 10^{-3}$ mbar) at the laser focus $\sim$1 cm above the oven. The sodium beam emitted from the $\sim$300-μm oven opening partially reduced volumetric averaging of the signal from the laser focus in a way characteristic of a transverse slit aperture [11] without using numerical or analytical deconvolution. The shortest (transform limited) pulse was created in the focus by adjusting the grating compressor in the laser amplifier. Electrons that were emitted from laser-ionized sodium and traveled down the μ-metal tube of the vacuum chamber in the direction of the electric field of the laser were detected with microchannel plates (MCPs) for time-of-flight and energy analysis.

III. RESULTS

Figure 2 displays three above-threshold ionization spectra measured for sodium vapor (Na I) with laser intensities ranging from 3.5×10^{12} to 8.8×10^{12} W/cm^2. The peaks in the spectra serve as probes of atomic level populations during the laser-atom interaction. A near-resonant two-photon transition

*nhart@physics.tamu.edu

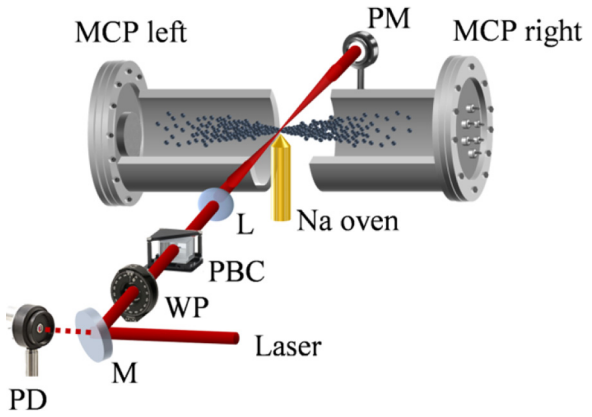

FIG. 1. The experimental apparatus and associated optics. (a) The experimental setup with (M) a steering mirror, half-wave plate (WP), polarizing beam-splitter cube PBC, lens (L), sodium oven, and power meter (PM) are shown along the beam path. A photodiode triggers the acquisition of electron counts from the chevron microchannel plates (MCP).

between the $3s$ ground state and $4s$ excited state favors the excitation of Rydberg P states $5p, 6p$, and $7p$ over F states $4f$, $5f$, and $6f$ [12,13]. Therefore, one-photon ionization from the $5p$ and $6p$ energy levels should provide the most prominent electron peaks at ≈ 0.76 and ≈ 1.03 eV, respectively. Rabi oscillations between the $3s$ ground state and the $3p$ first excited state [3] lead to the excitation of $3d$ and its subsequent ionization (see Figs. 2 and 3).

These peaks, along with all others below 1.55 eV, are shown in the plot one photon ($\hbar\omega \approx 1.55$ eV) in energy away from their respective bound state (-0.79 eV for $5p$, -0.51 eV for $6p$, and 0 eV for the continuum) and comprise the threshold peak (see Fig. 3). Ionization through the off-resonant $5p$ state is highly efficient. By fitting a Gaussian

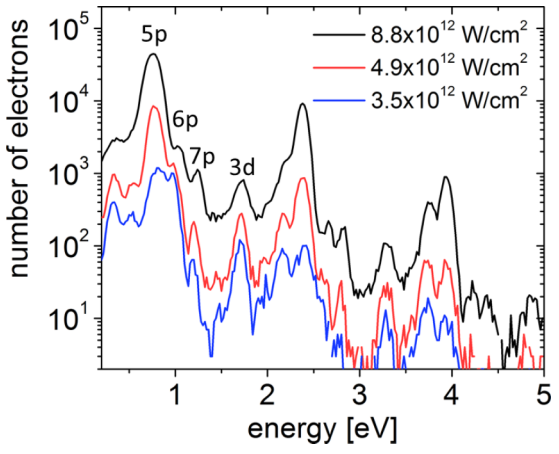

FIG. 2. Experimentally measured above-threshold ionization (ATI) spectra at laser intensities 3.5×10^{12} W/cm^2 (blue, lower curve), 4.9×10^{12} W/cm^2 (red, middle curve), and 8.8×10^{12} W/cm^2 (black, upper curve). The data show the first three photon orders of ATI peaks whose maximum values are located at 0.76, 2.4, and 3.9 eV. Substructures in the threshold peak owing to ionization through Rydberg states are labeled $5p$, $6p$, and $7p$, while the substructure labeled $3d$ belongs to the second-order peak.

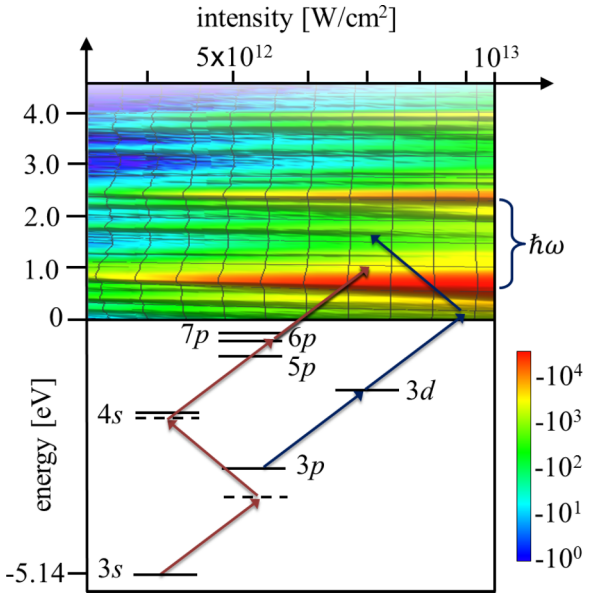

FIG. 3. Energy-level diagram for atomic sodium. The continuum shown is a surface plot of 30 experimentally measured ATI spectra. The ATI peaks are horizontal streaks and the laser intensity for each measurement is increasing towards the right with a range of $3.5 \times 10^{12} - 1.0 \times 10^{13}$ W/cm^2. Each diagonal arrow represents a photon absorption of approximately $\hbar\omega \approx 1.55$ eV in energy. Two possible quantum paths are shown whereby photon absorption produces ionization peaks.

to the $5p$ peaks at 0.76, 2.38, and 3.9 eV in the spectra for $I_0 = 5.1 \times 10^{12}$ W/cm^2 and comparing this with the entire electron yield, we estimate that 85% of the photoelectrons are ionized through the $5p$ intermediate state. It is worth noting that the Keldysh parameter at the over-the-barrier intensity ($I_{\mathrm{OTB}} = 2.79 \times 10^{12}$ W/cm^2) for Na is $\gamma = 3.98$, indicating that sodium ionization with our pulse parameters remains a multiphoton process even after surpassing the predicted saturation intensity [14]. Sustained multiphoton ionization beyond the over-the-barrier intensity was previously measured in lithium [15] and theoretically predicted for potassium [16]. In noble gases, plateaulike features in the above-threshold ionization (ATI) spectra associated with cutoff energies at 2 times and 10 times the ponderomotive energy of the laser field U_P are important measures for pulse characterization [17,18]. However, alkali metals present a particular challenge for observing such features because of the relatively low intensities needed for ionization. This is due to lower intensities having smaller cutoff energies, which leads to a shortage of peaks below the plateau cutoffs.

Figure 4 displays photoelectron yields of three subpeaks located at 0.76 eV($5p$), 0.98 eV($6p$), and 1.17 eV($7p$). According to lowest-order perturbation theory, the threshold subpeaks $5p$, $6p$, and $7p$ should have ionization yields that are proportional to the peak intensity I_0 to the fourth power ($Y \propto I_0^4$), which on a log-log plot produces a slope of 4 ($K = 4$). Yet we observe $K_{6p} = 1$ and $K_{5p} = 6$ (Fig. 4).

The difference between the intensity responses of these energy states is explained by the fact that as intensity increases, the dynamic Stark effect shifts $5p$ towards a three-photon

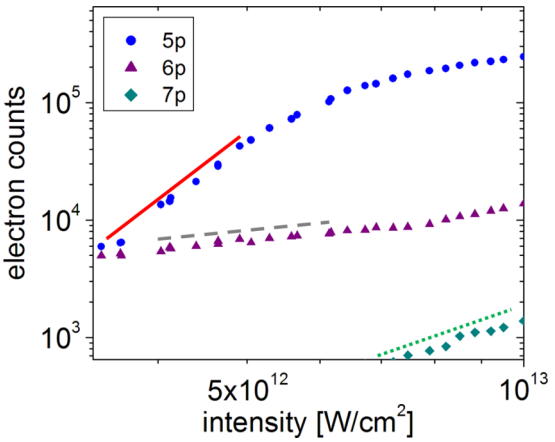

FIG. 4. Experimentally measured electron yields for ionization from the $5p$ (blue circles), $6p$ (purple triangles), and $7p$ (green diamonds) energy levels as a function of laser intensity. The maximum value of the $5p$, $6p$, and $7p$ peaks from the same data set as Figs. 2 and 3 are plotted. The red (solid) line has a slope of $K = 6$, the gray (dashed) line is for $K = 1$, and the green (dotted) line has $K = 2$.

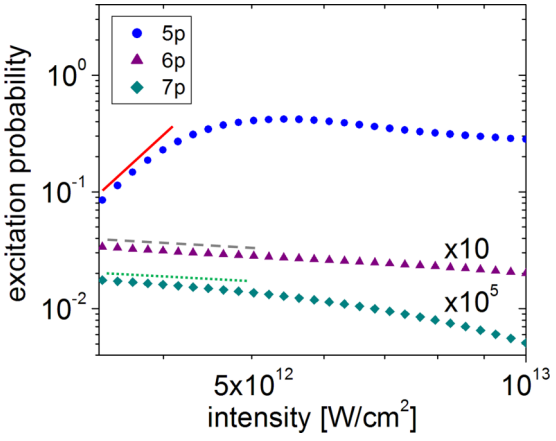

FIG. 5. Results of the resonance sampling (RS) model for three-photon absorption by $5p$, $6p$, and $7p$ levels as a function of the pulse peak intensity. The curves for $6p$ and $7p$ have been shifted vertically. The $5p$ excitation has a slope $K_{5p} = 8$ (red solid line), while $6p$ and $7p$ both have a slope $K \approx -0.5$ (gray dashed and green dotted lines, respectively). It should be noted that at low intensities ($<10^{11}$ W/cm^2), all three levels have a slope $K = 3$. The relatively low excitation probabilities for $6p$ and $7p$ suggest that REMPI is not the dominant mechanism for ionization through these states over the modeled intensity range.

resonance relative to the ground state, while $6p$ shifts away from this resonance. This enhanced rate of the electron population to the $5p$ state occurs through direct excitation, since the intermediate states $3p$ and $4s$ are detuned from the one- and two-photon resonances, respectively (see Fig. 3). The $7p$ state also shifts away from the three-photon resonance, but differs from $6p$ in that $7p$ lies outside of the three-photon bandwidth of the laser throughout the entire pulse. Therefore, resonant phenomena are not expected to dominate for this higher-energy state.

A qualitative understanding of the role REMPI plays in strong-field ionization may be gained from a simplified model where the multiphoton absorption rate is integrated in a classical two-state rate equation (see Fig. 5). Given that the sodium atom is initially in the $3s$ ground state, this model provides a qualitative estimate of the intensity-dependent population probability for a final excited state f (where f is either $5p$, $6p$, or $7p$) after the pulse has passed. For an instantaneous laser intensity I and three-photon cross section σ_3, the three-photon absorption rate is $W = \sigma_3 I^3$. The rate W for the $3s$ to f transition ($3s \rightarrow 3p \rightarrow 4s \rightarrow f$) is calculated using lowest-order perturbation theory [19]. We introduce the ac Stark shift $E^{(2)}(t)$ into the model by replacing the static three-photon detuning of the unperturbed atom, $\delta_f^* = 3\omega - \omega_{3s,f}$, with a dynamic detuning, $\delta_f = 3\omega - \omega_{3s,f} - E_f^{(2)}(t)/\hbar$, in the Lorentzian density of states function $\rho(\delta_f,\gamma_f)$ for level f in accordance with Mittleman [20]. The two-photon detuning for the $3s \rightarrow 4s$ transition and the one-photon detuning for the $3s \rightarrow 3p$ transition are $\delta_{4s} = 2\omega - \omega_{3s,4s} - E_{4s}^{(2)}(t)/\hbar$ and $\delta_{3p} = \omega - \omega_{3s,3p}$, respectively. If we let γ_{3p}, γ_{4s}, and γ_f equal the decay rates for levels $3p$, $4s$, and f, then the cross section for the four-level atom can be expressed as

$$\sigma_3 \approx A\rho(\delta_{3p},\gamma_{3p})\rho(\delta_{4s},\gamma_{4s})\rho(\delta_f,\gamma_f), \tag{1}$$

where A is a constant which does not affect the K value of the ionization process. For arbitrary δ and γ the normalized Lorentzian is

$$\rho(\delta,\gamma) = \frac{1}{\pi}\frac{\gamma/2}{(\delta)^2 + (\gamma/2)^2}. \tag{2}$$

To find the population in the final state, we integrate the two-state rate equations,

$$\frac{d}{dt}N_{3s} = -W(N_{3s} - N_f), \tag{3}$$

$$\frac{d}{dt}N_f = W(N_{3s} - N_f). \tag{4}$$

Because short pulses have large bandwidths, we average the rate W over the instantaneous bandwidth at each time step of the rate integration through the laser frequency ω. In our case, the linewidth γ_f of $\rho(\delta_f,\gamma_f)$ is much smaller than the laser bandwidth $\Delta\omega$. For this reason $\rho(\delta_f,\gamma_f)$ can be approximated as a delta function, which evaluates the rate W at a time-dependent frequency and laser pulse amplitude. We refer to this model as resonance sampling (RS). RS is particularly useful since it isolates the effect of directly populating an excited state associated with REMPI by excluding other excitation mechanisms.

Figure 5 shows that including the ac Stark shift into the rate qualitatively reproduces an increase in K_{5p} and a decrease in K_{6p}. The slope K_{5p} of the $5p$ excitation probability saturates when the resonance condition $\delta_{5p} \approx 0$ is satisfied at approximately 5×10^{12} W/cm^2. Contrarily, the slopes of $6p$ and $7p$ always decrease from their maximum value of $K = 3$, indicating a suppression of the excitation efficiency due to the ac Stark shift.

Two more-general observations can be made from the RS model. Firstly, all higher-energy P states ($6p$, $7p$, $8p$, etc.) should experience suppressed excitation since they will all

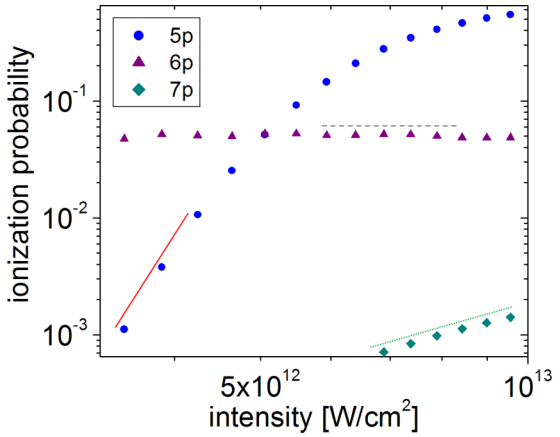

FIG. 6. Numerically simulated electron yields for ionization through $5p$ (blue circles), $6p$ (purple triangles), and $7p$ (green diamonds) energy levels as a function of laser intensity. As in Fig. 4, the maximum value of each peak is plotted. The red solid line refers to $K_{5p} = 14$, the gray dashed line is the result for $K_{6p} = 0$, and the green dotted line refers to $K_{7p} = 4$.

shift away from the three-photon resonance by roughly the ponderomotive energy. Moreover, if the intermediate level Stark-shifts completely out of the multiphoton bandwidth or is never in resonance during the pulse, then REMPI will not be a dominant ionization mechanism. In this case, intermediate excitation must occur by other means (i.e., Rabi oscillations [3]). Secondly, the greater the static detuning δ_f^* is above the unperturbed $5p$ state, the greater the efficiency of $5p$ excitation. This is because a larger detuning requires a higher intensity to create the Freeman resonance. And since the three-photon excitation rate W has a cubic dependence on intensity, the excitation efficiency is greatly enhanced. This intensity dependence is interesting, because it is the exact opposite of what is expected in the weak-field regime.

These trends are also confirmed by a numerical simulation solving the one- dimensional (1D) time-dependent Schrödinger equation (TDSE) for a sodiumlike atomic well (see Fig. 6). The simulation [21] uses a soft-core potential well,

$$V(x) = -\frac{ab}{\sqrt{x^2 + b^2}}, \tag{5}$$

where x is a spatial grid position, $a = 0.2411$, and $b = 3.6352$. In 1D, even and odd wave functions are produced. Therefore to compare results of the simulation with experimental data, we use even states as indicators of S state population and odd states as indicators of P state population. The values for parameters a and b reproduce the eigenvalues for the first three states of sodium $3s$, $3p$, and $4s$ to two significant figures. However, the higher-lying states do not closely reproduce the Rydberg energies. Therefore we chose an arbitrary set of odd intermediate states f using a photon energy of $\hbar\omega_s \approx 1.47$ eV, such that one level is slightly below the three-photon resonance, analogous to $6p$ in our experiment. The closest odd states above and below this near-$3\hbar\omega_s$ resonance are labeled $7p$ and $5p$ in Fig. 6. The simulation shows a dramatic enhancement of REMPI through a Freeman resonance at $5p$, as this level shifts into resonance. On the contrary, REMPI through $6p$ is suppressed, showing no intensity dependence over almost an order of magnitude. The $7p$ ionization is nonresonant throughout the entire calculation and does not appear to be involved in REMPI. Here also, selectivity of ionization through an intermediate level is attained at intensities exceeding the over-the-barrier intensity. In agreement with our model, the selective enhancement of REMPI arises from the larger static detuning δ_f^* relative to higher Rydberg states. In this case, an enhancement of the transition rate W correlates with a photon flux, which is more than 10 times greater for intensities at the $5p$ dynamic resonance ($\delta_{5p} \approx 0$) than for $6p$ ($\delta_{6p} \approx 0$). Moreover, integrating the electron probability from the $5p$ peaks of each ATI order indicates that this Freeman resonance can saturate the atomic ionization.

Here we see that laser-induced ac Stark shifts are efficient handles for controlling both the enhancement and suppression of ionization through various energy levels in the strong-field regime. This effect is present in experiments where the tunneling parameter is greater than unity ($\gamma > 1$) even when the laser intensity exceeds the over-the-barrier intensity of the atom. The near-multiphoton resonance from the ground state to a high-lying S state favors selective ionization through the Stark shift controlled P state and suppresses excitation of the higher angular momentum Rydberg states. While a special case, for the appropriate laser frequency, such an energy-level scheme can be found in many atoms and is a general characteristic of the alkali metals.

IV. CONCLUSION

In conclusion, a mechanism is described to account for selective excitation of a single energy state among a manifold of sodium Rydberg energy levels. By Stark-shifting the Rydberg states with the laser pulse intensity, we were able to single out a Freeman resonance that selectively enhances REMPI due to its large detuning δ_f^*. REMPI used in this manner was the dominant ionization mechanism, where greater than 80% of experimentally measured electrons were ionized through the target state $5p$. Simultaneously, REMPI through higher Rydberg states was suppressed by an ac Stark shift away from resonance. Moreover, the coherence of resonant ionization was maintained and was even optimal at intensities exceeding the over-the-barrier intensity of the atom. These results further the understanding of atom-specific REMPI and motivate future applications of strong-field coherent control.

ACKNOWLEDGMENTS

This work was supported by the Robert A. Welch Foundation Grant No. A1546 and the Qatar Foundation under Grant No. NPRP 5-994-1-172

[1] N. B. Delone and V. P. Kraĭnov, *Multiphoton Processes in Atoms* (Springer, Heidelberg, 2000), Vol. 13.

[2] K. J. LaGattuta, Phys. Rev. A **47**, 1560 (1993).

[3] W. Nicklich, H. Kumpfmüller, H. Walther, X. Tang, H. Xu, and P. Lambropoulos, Phys. Rev. Lett. **69**, 3455 (1992).

[4] B. Held, G. Mainfray, C. Manus, J. Morellec, and F. Sanchez, Phys. Rev. Lett. **30**, 423 (1973).
[5] C. Chang and P. Stehle, Phys. Rev. Lett. **30**, 1283 (1973).
[6] R. R. Freeman, P. H. Bucksbaum, H. Milchberg, S. Darack, D. Schumacher, and M. E. Geusic, Phys. Rev. Lett. **59**, 1092 (1987).
[7] G. N. Gibson, R. R. Freeman, and T. J. McIlrath, Phys. Rev. Lett. **69**, 1904 (1992).
[8] U. Eichmann, A. Saenz, S. Eilzer, T. Nubbemeyer, and W. Sandner, Phys. Rev. Lett. **110**, 203002 (2013).
[9] W. D. M. Lunden, P. Sándor, T. C. Weinacht, and T. Rozgonyi, Phys. Rev. A **89**, 053403 (2014).
[10] N. A. Hart, J. Strohaber, G. Kaya, N. Kaya, A. A. Kolomenskii, and H. A. Schuessler, Phys. Rev. A **89**, 053414 (2014).
[11] J. Strohaber, A. A. Kolomenskii, and H. A. Schuessler, J. Appl. Phys. **118**, 083107 (2015).
[12] M. Krug, T. Bayer, M. Wollenhaupt, C. Sarpe-Tudoran, T. Baumert, S. Ivanov, and N. Vitanov, New J. Phys. **11**, 105051 (2009).
[13] S. Lee, J. Lim, C. Y. Park, and J. Ahn, Opt. Express **19**, 2266 (2011).
[14] R. Potvliege and S. Vučić, Phys. Scr. **74**, C55 (2006).
[15] M. Schuricke, G. Zhu, J. Steinmann, K. Simeonidis, I. Ivanov, A. Kheifets, A. N. Grum-Grzhimailo, K. Bartschat, A. Dorn, and J. Ullrich, Phys. Rev. A **83**, 023413 (2011).
[16] F. Morales, M. Richter, S. Patchkovskii, and O. Smirnova, Proc. Natl. Acad. Sci. USA **108**, 16906 (2011).
[17] G. G. Paulus, F. Grasbon, H. Walther, P. Villoresi, M. Nisoli, S. Stagira, E. Priori, and S. De Silvestri, Nature **414**, 182 (2001).
[18] D. B. Milošević, G. G. Paulus, D. Bauer, and W. Becker, J. Phys. B: At., Mol. Opt. Phys. **39**, R203 (2006).
[19] R. W. Boyd, *Nonlinear Optics* (Academic, Waltham, MA, 2008).
[20] M. H. Mittleman, *Introduction to the Theory of Laser-Atom Interactions* (Springer, New York, 1993), p. 153.
[21] G. G. Paulus, W. Nicklich, H. Xu, P. Lambropoulos, and H. Walther, Phys. Rev. Lett. **72**, 2851 (1994).